

# Structural evolution, GFA and mechanical properties of Zr-Cu-Al ternary metallic-glass system: A molecular dynamics simulation study

**Mohammadreza Falaki**

Department of Materials Science and Engineering, Sharif University of Technology, Azadi Avenue, P. O. Box 11155-9466, Tehran, Iran

**Mir Alireza Faghani Tolon**

Department of Materials Science and Engineering, Sharif University of Technology, Azadi Avenue, P. O. Box 11155-9466, Tehran, Iran

## Abstract

Metallic glass (MG) structures have gained significant attention due to their unique properties. These materials mostly exhibit short-range order in the form of polyhedral clusters, which greatly influence the final properties, stability of the metallic glass and higher glass formation. In this study, classical molecular dynamics simulations are employed to calculate the glass transition temperature of a ternary  $Zr_{47}Cu_{46}Al_7$  structure, then analyzing the atomic structure at various temperatures during quenching to observe and investigate the short-range order and the population of Voronoi polyhedra. Subsequently, the mechanical properties of the structure are evaluated through tensile testing. The results demonstrate that the present structure exhibits higher glass stability and desirable mechanical properties, including significant yield stress, compared to other atomic percentages of the same composition and the binary CuZr MGs.

**Keywords:** Molecular dynamics simulation, Metallic glasses, GFA, Short-range order, Voronoi analysis, Mechanical properties.

## 1. Introduction

Metallic glasses (MGs) have garnered significant attention due to their exceptional yielding strength, excellent corrosion resistance, and diverse applications in structural and biomedical fields [1,2]. Their potential as advanced structural materials has further fueled interest [3]. Recent advancements in science and technology have accelerated the development of new MG materials, enabling more successful synthesis than in previous years. Among these, CuZr-based MGs have revitalized research into MG structures [4–6]. The liquid-glass phase transition in binary Zr–Cu alloys is well-documented, occurring across a broad compositional range during rapid solidification [7]. Due to their unique properties and extensive application potential, numerous experimental and theoretical studies have been conducted to explore the atomic structures, mechanical properties, and topological order of these binary alloys [8–10]. The critical thickness of binary Cu–Zr alloys has been typically limited to about 1–1.5 mm, but incorporating elements such as Al, Ag and/or Ni can extend this critical thickness to up to 14 mm [11]. Particularly, adding Ag and Al (usually in amounts of 10% or less) to Cu–Zr alloys significantly enhances their glass-forming ability (GFA) and stabilizes the supercooled liquid [12, 13].

molecular dynamics (MD) simulations have been extensively used to examine the effects of Al and Ag on Zr–Cu binary alloys [13–17]. These studies, though insightful, often rely on a limited set of analytical methods. Despite intensive research on the atomic structures of Zr–Cu–Al ternary metallic liquid and glass, the structural evolution and glass transition properties of these systems remain not fully understood. To address these gaps, in this research used MD simulations to elucidate the structural evolution and glass formation properties of Zr<sub>47</sub>Cu<sub>46</sub>Al<sub>7</sub> metallic liquid and glass. MD simulations are particularly effective in overcoming the challenges of supercooled liquids crystallizing during rapid solidification. Here, the primary goal is to deepen the understanding of these systems, by examining their GFA properties and structural characteristics in both liquid and supercooled states as the temperature decreases. Additionally, aim is to compare the effects of Al (at 7% atomic) with the CuZr binary system across a wide temperature range, thereby contributing to the literature with structural analyses of the new ternary alloy. In this study, meticulously investigated the structural evolution and glass formation processes of Zr<sub>47</sub>Cu<sub>46</sub>Al<sub>7</sub> metallic liquid and glass during cooling, utilizing the embedded atom method (EAM) combined with MD simulations. The results are statistically analyzed using structural factors (SF), pair distribution functions (PDF), and Voronoi polyhedra (VP) methods. also discussed the local structural similarities and differences between the ternary and binary (from the literature) in detail in the following sections. Also, the mechanical properties of Zr<sub>47</sub>Cu<sub>46</sub>Al<sub>7</sub> evaluated with tensile test at 300 K and different strain rates and the results compared to the binary system available in the literature.

The atomic structure level of Zr<sub>47</sub>Cu<sub>46</sub>Al<sub>7</sub> metallic liquid and glass have been investigated by using EAM-MD simulations, and the evolution of their local atomic structures during the cooling process have been characterized by SF, PDF analysis [18] and VP method [19]. The structure factors,  $S(q)$ , are related to the PDF,  $g(r)$ , by

$$S(q) = 1 + 4\pi\rho \int r^2 \sin qr / qr (g(r) - 1) dr \quad (1)$$

where  $\rho$  is the averaged number density of the system. Total PDF,  $g(r)$ , and partial PDF functions (pPDF),  $g_{ij}(r)$  are defined as follows:

$$g(r) = V/N^2 \left\langle \sum_i^N \sum_{j=i}^N \delta(r - r_{ij}) \right\rangle \quad (2)$$

$$g_{\alpha\beta}(r) = V / N_{\alpha}N_{\beta} \left\langle \sum_i^N \sum_{j=i}^N \delta(r - r_{ij}) \right\rangle \quad (3)$$

where  $N_{\alpha}$  and  $N_{\beta}$  represent the number of atoms of type  $\alpha$  and type  $\beta$ , respectively, in a system with  $N$  atoms.  $V$  and  $\delta(r - r_{ij})$  are the volume of the simulation box and the Dirac delta function, respectively. Both the pPDFs and the total PDFs are calculated and presented in the next sections.

## 2. Simulation method

Classical MD simulations were performed to investigate the structural evolution and mechanical properties of the alloy. Periodic boundary conditions were applied to a system containing 8192 atoms in all directions. The simulations were conducted using the EAM force field and the LAMMPS [20] software. Open visualization tool [21] (OVITO) software was employed to visualize and analysis the MD simulation results. Initially, the atoms were arranged in a body-centered cubic (BCC) crystal structure and minimized using the Conjugate Gradient (CG) algorithm. The structure was then heated to 1800 K and equilibrated for 40 nanoseconds under the NPT ensemble without applying external pressure at the same temperature to achieve equilibrium. Subsequently, the system was quenched with a cooling rate of  $10^{12}$  K/s to form an amorphous structure. The resulting structure was then equilibrated for 20

nanoseconds at 300 K under the NPT ensemble to achieve thermal equilibrium. Finally, the structure was minimized using the CG algorithm to obtain the final structure. Tensile tests were then performed on the sample in the X-direction at four different strain rates  $10^9 \text{ s}^{-1}$ ,  $5 \times 10^9 \text{ s}^{-1}$ ,  $10^{10} \text{ s}^{-1}$  and  $5 \times 10^{10} \text{ s}^{-1}$ , respectively. The pressures on the Y and Z direction were kept at zero. The full-procedure of the simulation is shown in "Figure 1".

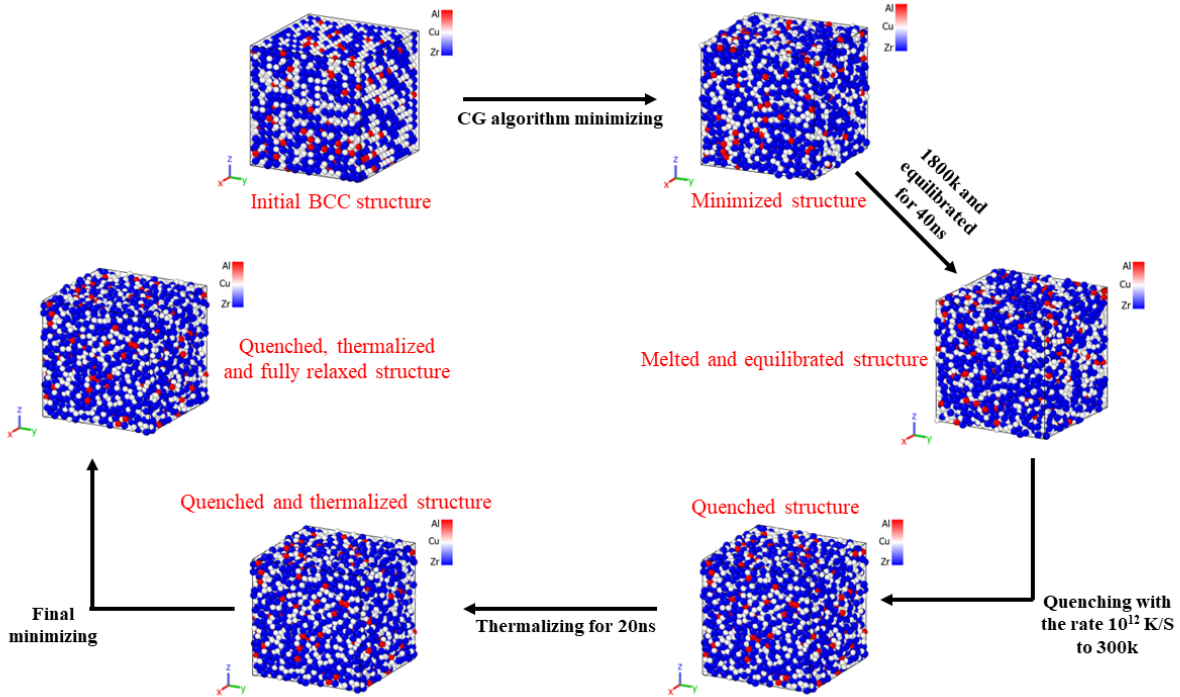


Figure (1) Schematic diagram of the simulation process.

### 3. Results and discussion

#### 3.1 Glass transition temperature, $T_g$

"Figure 2" illustrates the evolution of the volume of  $\text{Zr}_{47}\text{Cu}_{46}\text{Al}_{17}$  metallic liquid and glass as a function of temperature during cooling. The volume-temperature curve exhibit no abrupt changes due to temperature decreases, indicating the absence of first-order phase transitions, such as crystallization. As observed in Figure 2, the volume decreases almost linearly from 1500 K to 900 K with the decrease in temperature. Below 900 K, the rate of volume reduction slows, and the decline continues nearly linearly but with a different slope in the 850 K to 300 K range. The intersection of red lines determines the glass transition temperature  $T_g$  [22]. Here, the  $T_g$  determined as 836 K, which is way above the reported  $T_g = 650 \text{ K}$  for CuZr binary system by Wei et al [23].

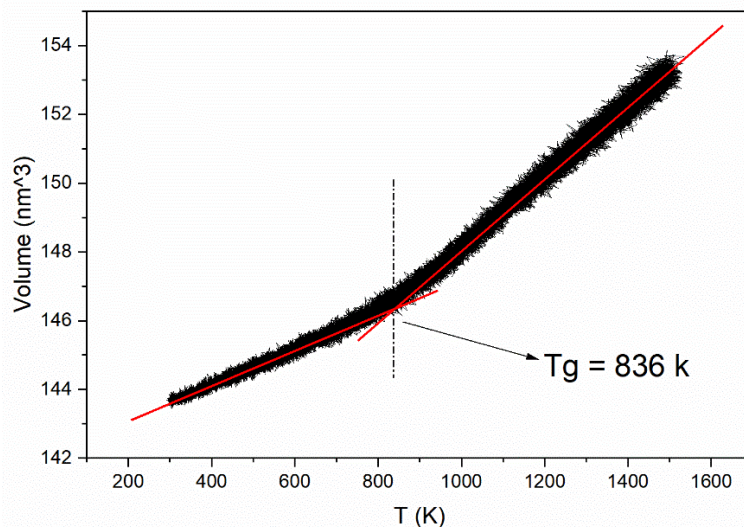


Figure (2) The evolution of the volume of Zr47Cu46Al7 metallic liquid and glass as a function of temperature.

### 3.2 Pair distribution functions (PDFs) and and structure analysis

The evolution of the total PDFs for Zr47Cu46Al7 metallic liquid and glass obtained in the temperature range from 1800 K to 300 K during rapid cooling is shown in "Figure 3". The variations of all PDF curves are very similar. While the peaks of the PDF curves obtained at high temperature ranges show typical characteristics of liquid structures, they show a typical characteristics of glassy structures at lower temperatures. Due to the decreasing temperature, the widths of the first peaks of the PDFs contract and their height increases. This may be attributed to the fact that the short range order (SRO) and medium range order (MRO) continues to increase with decreasing temperature and that the glasses have a higher degree of SRO formation than liquids. In addition, as the temperature decreases further, humps have appeared to the right and left of the first maximum peaks of the total PDF curves obtained, indicating a significant change in systems at low temperatures.

"Figure 4" also illustrates the evolution of the partial pair distribution functions, which exhibits behavior and analysis similar to Figure 3. In "Figure 4 and 5", as the temperature decreases, the first peak of the copper-aluminum (Cu-Al) pair records a relatively higher height compared to other pairs, indicating the formation of stable icosahedra at lower temperatures, centered around copper or aluminum. The peak height is higher than those reported by Celtek et al. [24] for binary CuZr and ternary Zr47.5Cu47.5Al5 system (6.4). This contributes to the structure achieving a great short-range order compared to Zr-Cu, or Zr-Cu-Al systems with other atomic percentages, because of the optimal Al addition.

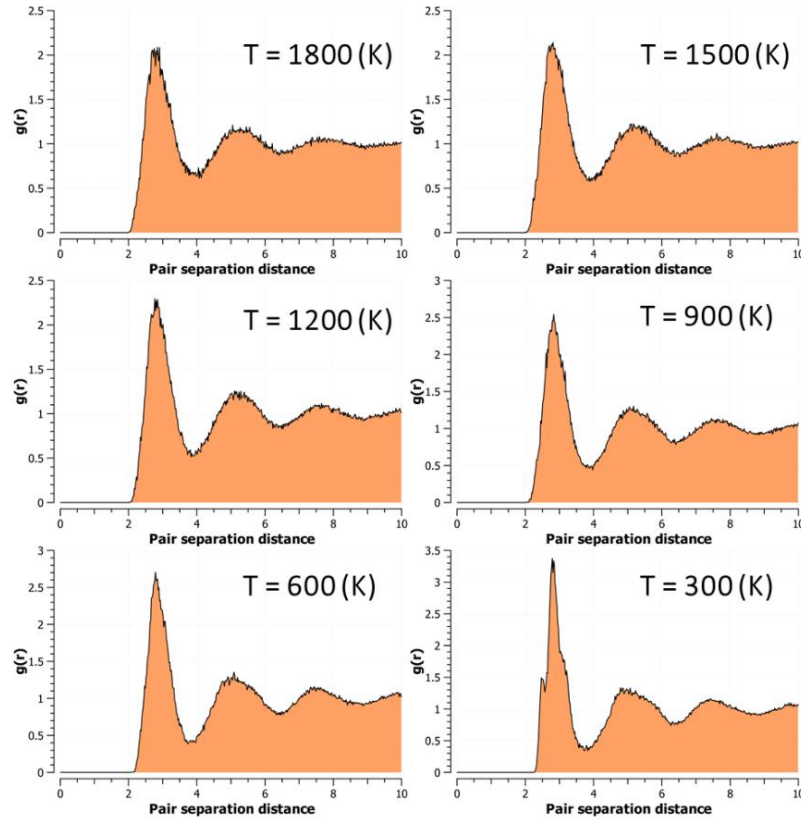


Figure (3) The evolution of the total PDFs during the cooling process at different temperatures.

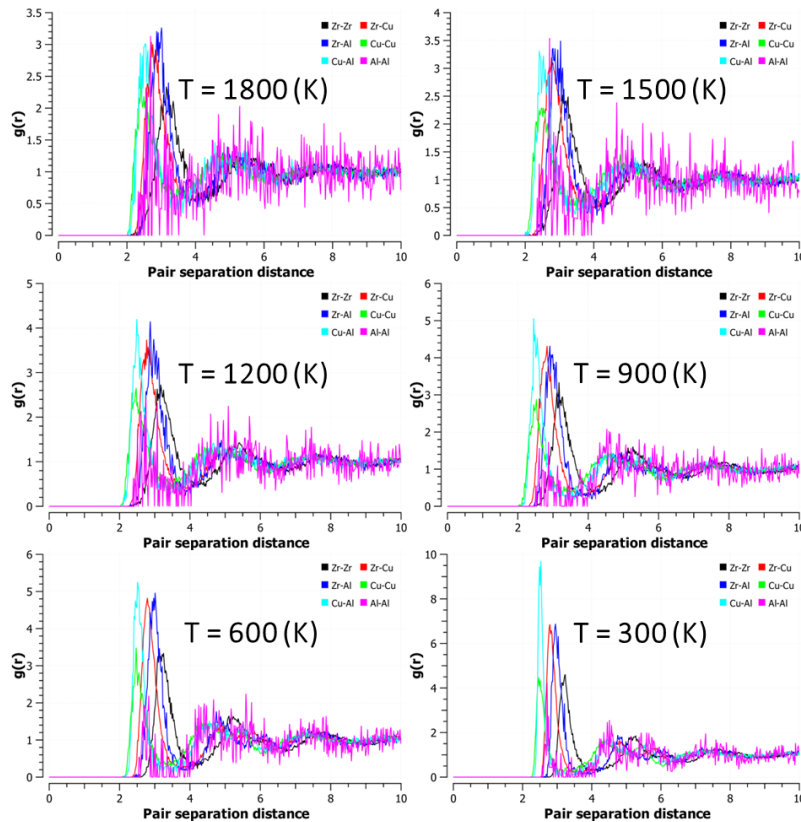


Figure (4) The evolution of the partial PDFs during the cooling process at different temperatures.



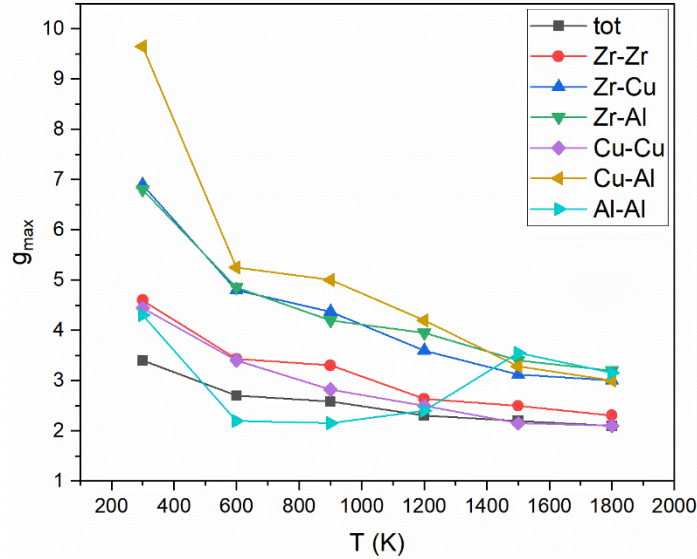


Figure (5) Evolution of the heights of the partial and total PDFs during the cooling process at different tempratures.

In order to see in detail which kind of clusters contributed more to the development of SRO/MRO in the MG, used the grouping method previously proposed by Cheng et al. [25] and Hwang et al. [26]. They divided Voronoi Polyhedras (VPs) into three categories. According to this VP groups; icosahedral-like clusters consist of  $\langle 0, 0, 12, x \rangle$ ,  $\langle 0, 1, 10, x \rangle$  and  $\langle 0, 2, 8, x \rangle$  VPs ( $\langle 0, 0, 12, 0 \rangle$  for full-icosahedra), mixed clusters  $\langle 0, 3, 6, x \rangle$  and  $\langle 0, 3, 7, x \rangle$  VPs and crystal-like clusters  $\langle 0, 4, 4, x \rangle$  VPs and in where  $x$  is a typical number between 0 and 6. The results obtained at 300 K for the MG have been classified according to this method and shown in "Figure 6". The local structure of the MG is dominated by the icosahedral-like symmetry. Given the distribution of VPs shown in Fig. 6, the fractions of each categories of VPs for the Zr<sub>47</sub>Cu<sub>46</sub>Al<sub>7</sub> MG are ~37.8%, ~9.2% and ~1.7%, respectively.

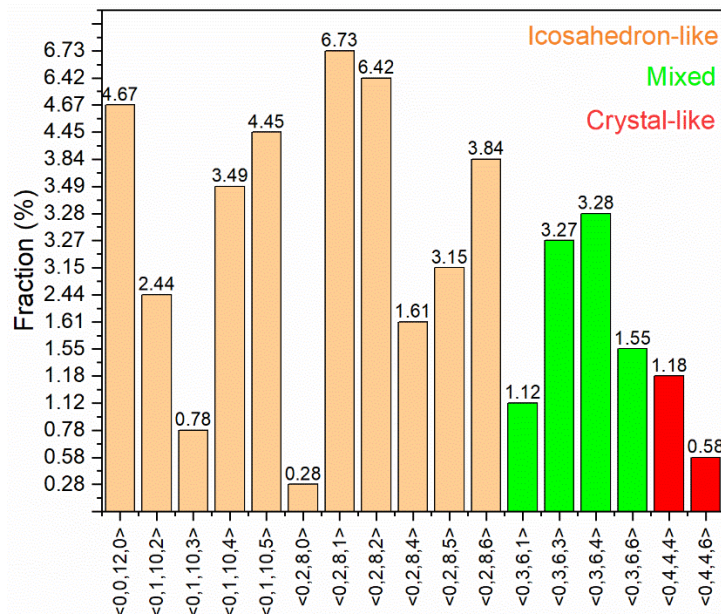


Figure (6) Fraction of the most common voronoi polyhedra indices in the metallic glass at 300 K.



"Figure 7" shows the full-icosahedrons (FI) with index  $\langle 0,0,12,0 \rangle$ , their arrangement and distribution within the structure at different temperatures. It is evident that as the temperature decreases and passes through the molten region (below 1000 K), the rate of increase in icosahedrons becomes very high and their spread encompasses the entire structure. Therefore, they form an interconnected skeleton within the structure. At room temperature (RT), approximately 370 complete icosahedrons are present within the structure. "Figure 8" illustrates the number of complete icosahedrons as a function of temperature. As previously mentioned, upon passing from the molten state during cooling, the rate of production of complete icosahedron suddenly increases from around 1000 K, resulting in a steeper curve.

"Figure 9a" shows the distribution of icosahedra according to the central atom as well as the atomic structure. The color coding of the atoms is based on the fifth Voronoi index, where the number 12 indicates a complete icosahedron, and lower numbers represent distorted icosahedra. In this figure, red atoms are the centers of complete icosahedra. Copper, due to its smaller atomic radius compared to the other two elements, tends to form more icosahedra, thereby reducing the system's energy. Consequently, a large fraction of the icosahedra are centered around copper, with icosahedra also forming around aluminum and zirconia. "Figure 9b" presents only the distribution of complete icosahedra according to their central atom, along with the atomic structure. Blue atoms represent copper, and red atoms represent aluminum. After the system stabilizes at ambient temperature, no complete icosahedra form around zirconia, and only those around copper and aluminum are found. As mentioned earlier, most of these icosahedra are centered around copper. However, aluminum also plays a significant role in stabilizing the glass because it forms a considerable number of icosahedra around itself or connects to a Cu-centered icosahedra with ease.

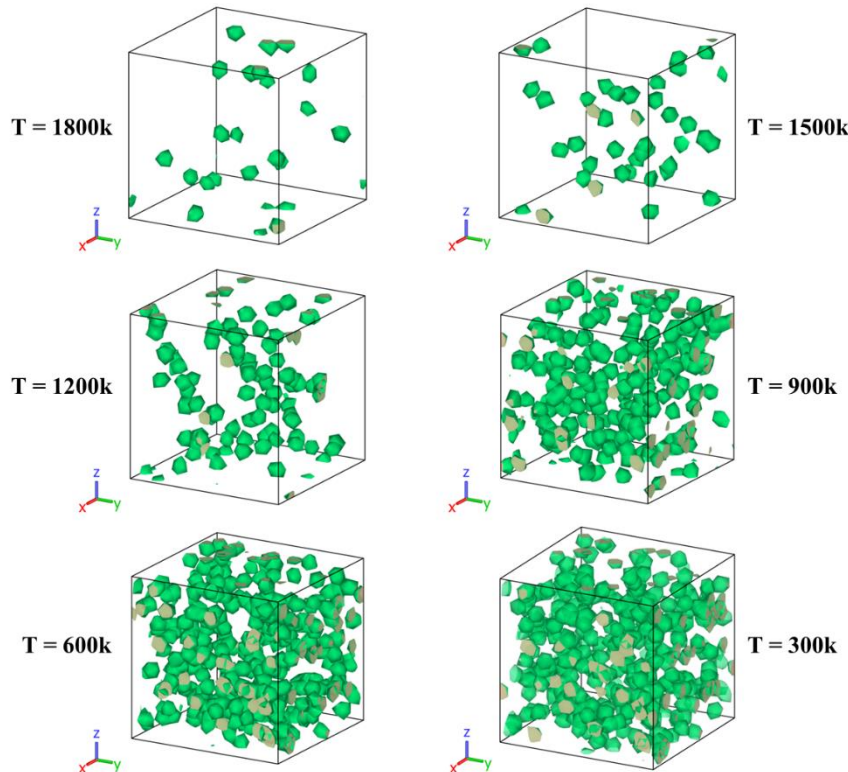


Figure (7) Evolution of the full icosahedrons and their arrangement in the structure at different tempratures.

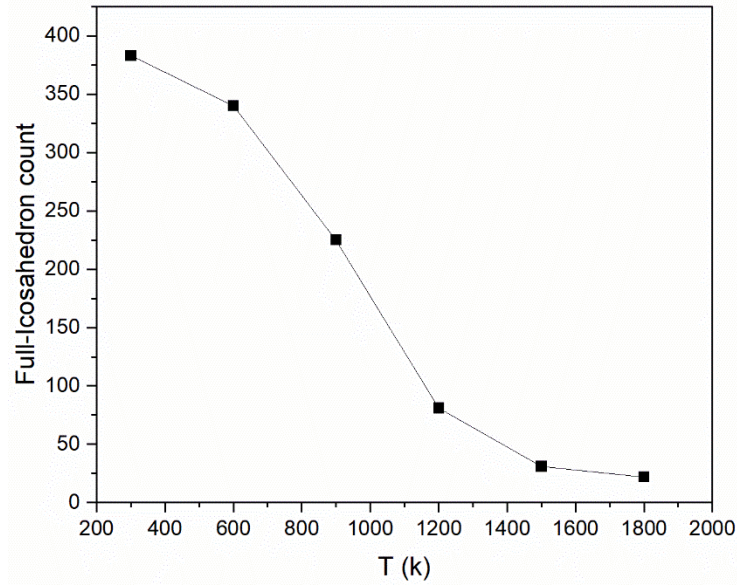


Figure (8) Full-icosahedron count at different temperatures.

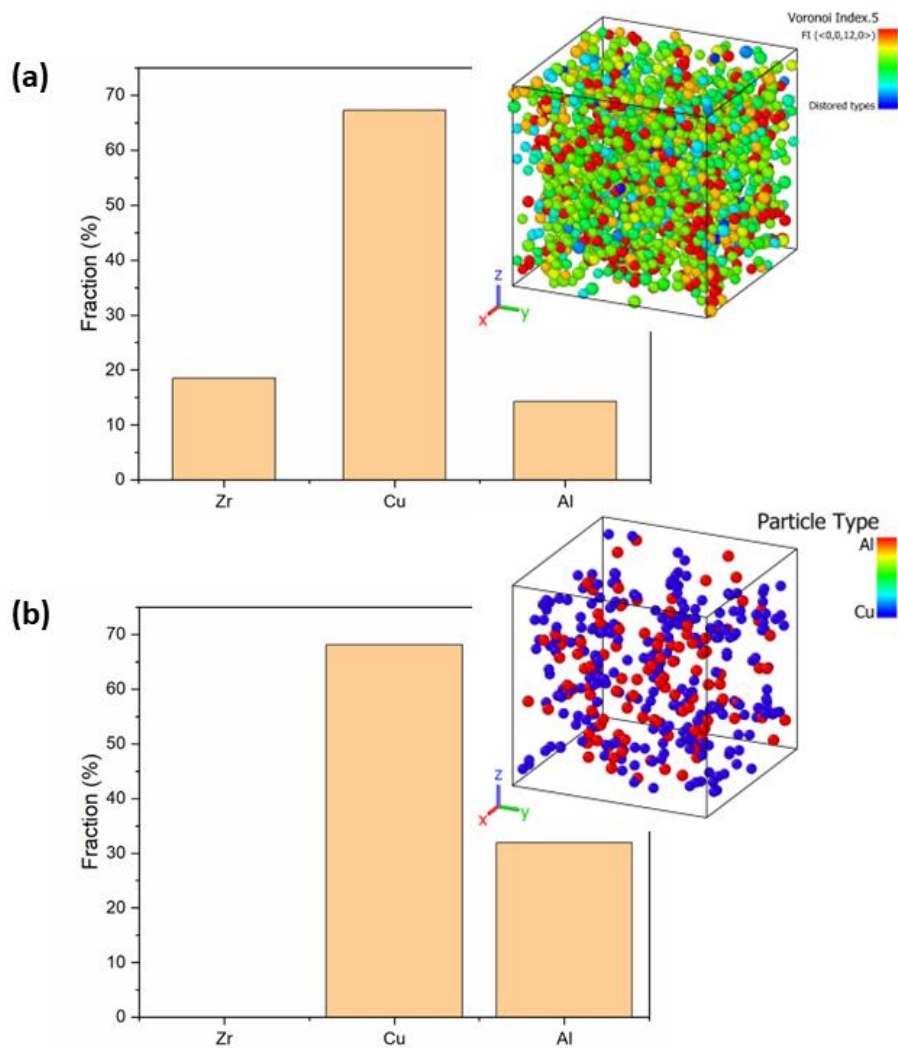


Figure (9) Fraction of the (a) icosahedrons and (b) full icosahedrons in the structure according to their central atom.





### 3.3 Mechanical properties

Figures 10 to 13 show the stress-strain curves resulting from tensile tests on metallic glass at different strain rates at 300 K. As previously demonstrated, aluminum has a significant impact on improving the glass-forming ability, and it also greatly influences the mechanical properties. The structure obtained in this study requires more force to overcome and deform due to the higher number of continuous full-icosahedra and the symmetric nature of the icosahedra. Additionally, a substantial amount of energy is required to break the Cu-Zr bonds within the icosahedra, which contributes to the high strength and yield stress of this glassy alloy. The peak and yield stress in the glass structure of the present study are significantly higher than the values reported by Liang et al. [27] for the binary CuZr system (1.61 GPa) or the ternary system with different atomic percentages from this study (1.9 GPa for Zr<sub>47.5</sub>Cu<sub>47.5</sub>Al<sub>15</sub>).

It is evident that with an increase in strain rate, the yield stress slightly increases due to the properties and nature of the formed shear bands, as clearly observed in Figures 10 to 13. In Figure 14a, the values of yield stress and ultimate tensile stress as a function of strain rate are calculated and presented. As explained, with an increase in strain rate, the yield stress increases almost linearly from around 2 GPa to about 3.5 GPa. Similarly, the ultimate tensile strength also increases from around 2.5 GPa to 3.5 GPa as the strain rate increases, following the same trend as the yield stress. In Figure 14b, the calculated values of Young's modulus are presented, which are considerably higher compared to the values reported by Deb Nath [28] for Zr<sub>65</sub>Cu<sub>35</sub>Al<sub>10</sub> (41 GPa).

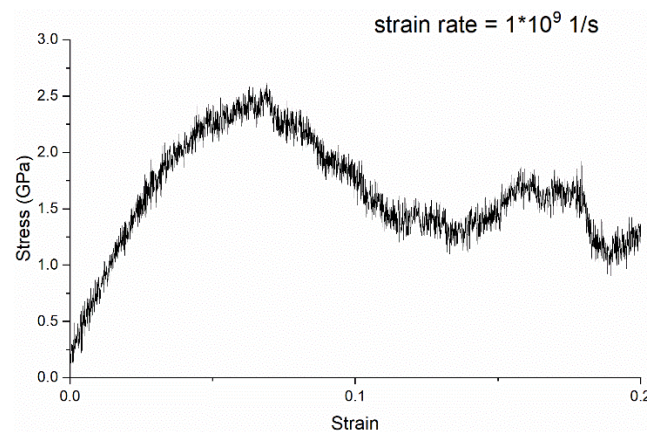


Figure (10) Stress strain curve for the metallic glass at  $10^9 \text{ s}^{-1}$  strain rate.

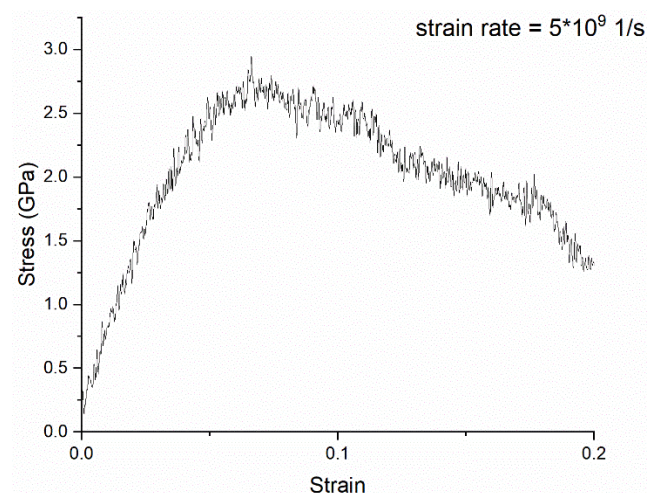


Figure (11) Stress strain curve for the metallic glass at  $5 \times 10^9 \text{ s}^{-1}$  strain rate.

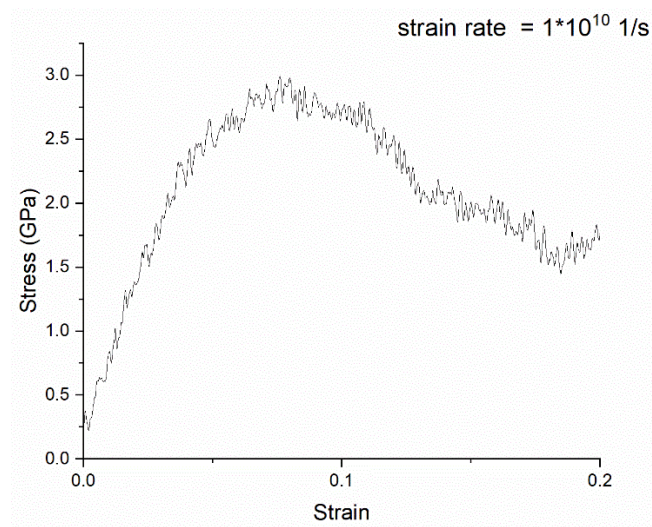


Figure (12) Stress strain curve for the metallic glass at  $10^{10} \text{ s}^{-1}$  strain rate.

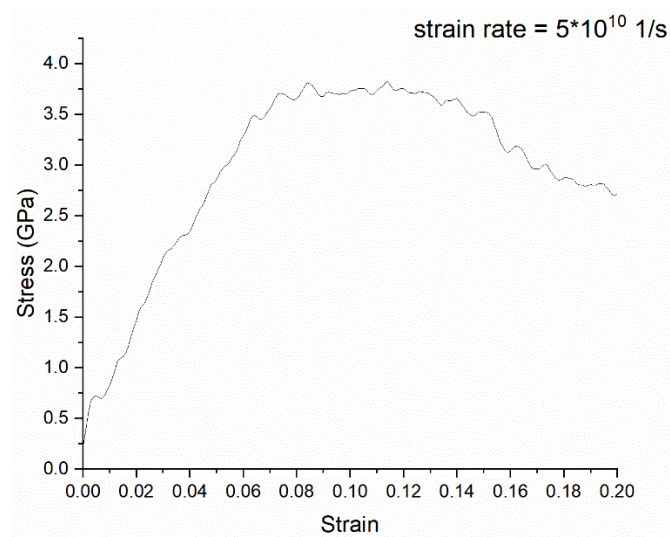


Figure (13) Stress strain curve for the metallic glass at  $5 \times 10^{10} \text{ s}^{-1}$  strain rate.

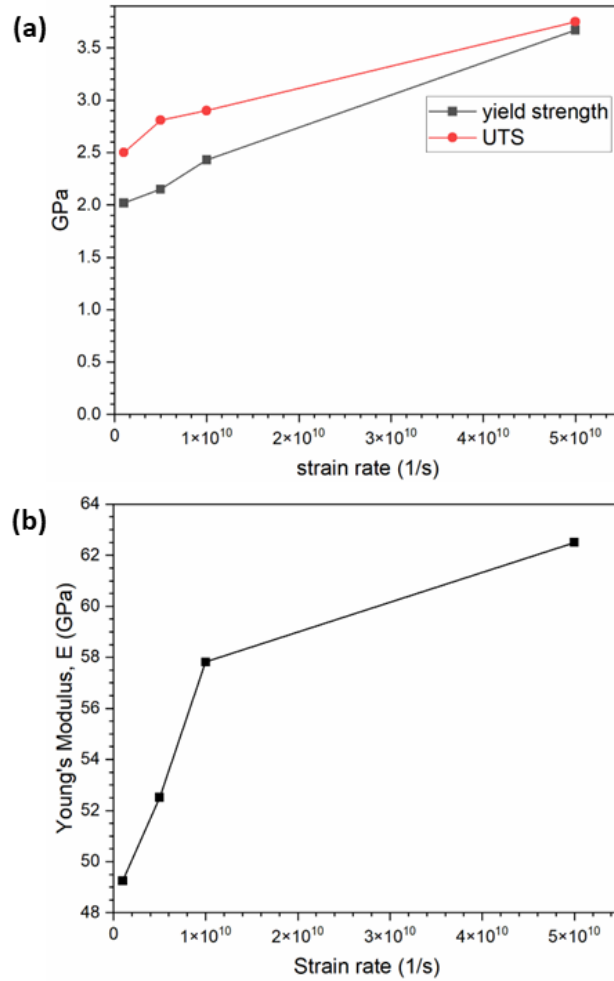


Figure (14) Calculated (a) yield strength and UTS (b) young's module at different strain rates.

## Conclusion

This study provides a comprehensive analysis of the structural evolution and mechanical properties of Zr<sub>47</sub>Cu<sub>46</sub>Al<sub>7</sub> metallic glass. Findings highlight the significant role of aluminum in enhancing both the glass-forming ability and the mechanical properties of this alloy.

1. The volume-temperature curves indicated no abrupt changes, suggesting the absence of first-order phase transitions such as crystallization. As the temperature decreased, the volume reduction proceeded almost linearly, with a noticeable change in slope around 850 K. This behavior underscores the stability of the amorphous structure during cooling and higher GFA relative to CuZr binary systems (650 K).

2. The pair distribution function analysis revealed that, as the temperature dropped, the first peak for the copper-aluminum pair became significantly higher than for other pairs. This indicates the formation of stable icosahedra centered around copper or aluminum at lower temperatures, contributing to a well-defined short-range order within the structure.

3. The distribution of icosahedra, as depicted in the figures, showed that aluminum played a crucial role in forming a high number of continuous icosahedra. This arrangement led to an interconnected skeleton within the structure, enhancing its overall stability. Copper, due to its smaller atomic radius, also contributed significantly by forming a large number of icosahedra, which reduced the system's energy and improved its stability.

4. The tensile tests demonstrated that the structure required substantial force to deform, owing to the symmetric nature of the icosahedra and the high energy required to break the copper-aluminum bonds. The peak and yield stress of the glass alloy in this study were markedly higher than those reported for other compositions, indicating superior mechanical properties. The strain rate dependency further illustrated that the yield stress and ultimate tensile strength increased linearly with the strain rate, confirming the robustness of the material.

In summary, aluminum significantly enhances the glass-forming ability and mechanical properties of the Zr<sub>47</sub>Cu<sub>46</sub>Al<sub>7</sub> metallic glass. The presence of aluminum leads to the formation of numerous stable icosahedra and

more icosahedron SRO, which play a pivotal role in maintaining the structural integrity and improving the strength of the glass alloy. These findings contribute valuable insights into the design and optimization of high-performance metallic glasses for various applications.

## References

- [1] A. Inoue, A. Takeuchi, Recent development and application products of bulk glassy alloys, *Acta Mater.* (2011) 2243–2267, <https://doi.org/10.1016/j.actamat.2010.11.027>.
- [2] M. Chen, A brief overview of bulk metallic glasses, *NPG Asia Mater.* 3 (2011) 82–90, <https://doi.org/10.1038/asiamat.2011.30>.
- [3] I. Kaban, P. Jovari, B. Escher, D.T. Tran, G. Svensson, M.A. Webb, T.Z. Regier, V. Kokotin, B. Beuneu, T. Gemming, J. Eckert, Atomic structure and formation of CuZrAl bulk metallic glasses and composites, *Acta Mater.* 100 (2015) 369–376, <https://doi.org/10.1016/j.actamat.2015.08.060>.
- [4] D. Xu, B. Lohwongwatana, G. Duan, W.L. Johnson, C. Garland, Bulk metallic glass formation in binary Cu-rich alloy series – Cu100- xZrx (x=34, 36, 38.2, 40 at.%) and mechanical properties of bulk Cu64Zr36 glass, *Acta Mater.* 52 (2004) 2621–2624, <https://doi.org/10.1016/j.actamat.2004.02.009>.
- [5] D. Wang, Y. Li, B.B. Sun, M.L. Sui, K. Lu, E. Ma, Bulk metallic glass formation in the binary Cu–Zr system, *Appl. Phys. Lett.* 84 (2004) 4029–4031, <https://doi.org/10.1063/1.1751219>.
- [6] G. Duan, D. Xu, Q. Zhang, G. Zhang, T. Cagin, W.L. Johnson, W.A. Goddard, Molecular dynamics study of the binary Cu46Zr54 metallic glass motivated by experiments: glass formation and atomic-level structure, *Phys. Rev. B Condens. Matter* 71 (2005) 1–9, <https://doi.org/10.1103/PhysRevB.71.224208>.
- [7] N. Mattern, a. Schops, U. Kühn, J. Acker, O. Khvostikova, J. Eckert, Structural behavior of CuxZr100-x metallic glass (x = 35-70), *J. Non-Cryst. Solids* 354 (2008) 1054–1060, <https://doi.org/10.1016/j.jnoncrysol.2007.08.035>.
- [8] N. Mattern, P. Jovari, I. Kaban, S. Gruner, a. Elsner, V. Kokotin, H. Franz, B. Beuneu, J. Eckert, Short-range order of Cu-Zr metallic glasses, *J. Alloys Compd.* 485 (2009) 163–169, <https://doi.org/10.1016/j.jallcom.2009.05.111>.
- [9] J. Antonowicz, a. Pietnoczka, W. Zalewski, R. Bacewicz, M. Stoica, K. Georgarakis, a.R. Yavari, Local atomic structure of Zr-Cu and Zr-Cu-Al amorphous alloys investigated by EXAFS method, *J. Alloys Compd.* 509 (2011) S34–S37, <https://doi.org/10.1016/j.jallcom.2010.10.105>.
- [10] X.D. Wang, Q.K. Jiang, Q.P. Cao, J. Bednarcik, H. Franz, J.Z. Jiang, Atomic structure and glass forming ability of Cu46Zr46Al8 bulk metallic glass, *J. Appl. Phys.* 104 (2008), 093519, <https://doi.org/10.1063/1.3009320>.
- [11] W. Zhang, A. Inoue, High glass-forming ability and good mechanical properties of new bulk glassy alloys in Cu–Zr–Ag ternary system, *J. Mater. Res.* 21 (2006) 234–241, <https://doi.org/10.1557/jmr.2006.0020>.
- [12] Q. Wang, C. Dong, J. Qiang, Y. Wang, Cluster line criterion and Cu–Zr–Al bulk metallic glass formation, *Mater. Sci. Eng.* 449–451 (2007) 18–23, <https://doi.org/10.1016/j.msea.2006.02.271>.
- [13] Y.Q. Cheng, E. Ma, H.W. Sheng, Atomic level structure in multicomponent bulk metallic glass, *Phys. Rev. Lett.* 102 (2009) 1–4, <https://doi.org/10.1103/PhysRevLett.102.245501>.
- [14] C.C. Wang, C.H. Wong, Structural properties of ZrxCu90-xAl 10 metallic glasses investigated by molecular dynamics simulations, *J. Alloys Compd.* 510 (2011) 107–113, <https://doi.org/10.1016/j.jallcom.2011.07.110>.

- [15] V. Kokotin, H. Hermann, J. Eckert, Computer simulation of the matrix–inclusion interphase in bulk metallic glass based nanocomposites, *J. Phys. Condens. Matter* 23 (2011) 425403, <https://doi.org/10.1088/0953-8984/23/42/425403>.
- [16] Y. Hu, T.J. Rupert, Atomistic modeling of interfacial segregation and structural transitions in ternary alloys, *J. Mater. Sci.* 54 (2019) 3975–3993, <https://doi.org/10.1007/s10853-018-3139-x>.
- [17] S. Senturk Dalgic, M. Celtek, Liquid -to-glass transition in bulk glass-forming Cu55-xZr45Agx alloys using molecular dynamic simulations, *EPJ Web Conf.* 15 (2011), 03009, <https://doi.org/10.1051/epjconf/20111503009>.
- [18] J.D. Honeycutt, H.C. Andersen, Molecular dynamics study of melting and freezing of small lennard- jones clusters, *J. Phys. Chem.* 91 (1987) 4950–4963, <https://doi.org/10.1021/j100303a014>.
- [19] G. Voronoi, New parametric applications concerning the theory of quadratic forms - second announcement, *J. für die Reine Angewandte Math. (Crelle's J.)* 134 (1908) 198–287.
- [20] LAMMPS - a flexible simulation tool for particle-based materials modeling at the atomic, meso, and continuum scales, A. P. Thompson, H. M. Aktulga, R. Berger, D. S. Bolintineanu, W. M. Brown, P. S. Crozier, P. J. in 't Veld, A. Kohlmeyer, S. G. Moore, T. D. Nguyen, R. Shan, M. J. Stevens, J. Tranchida, C. Trott, S. J. Plimpton, *Comp Phys Comm*, 271 (2022) 10817.
- [21] A. Stukowski, Visualization and analysis of atomistic simulation data with OVITO the Open Visualization Tool, *Model. Simulat. Mater. Sci. Eng.* 18 (2010), 015012, <https://doi.org/10.1088/0965-0393/18/1/015012>.
- [22] J.J. Han, W.Y. Wang, X.J. Liu, C.P. Wang, X.D. Hui, Z.K. Liu, Effect of solute atoms on glass-forming ability for Fe–Y–B alloy: an ab initio molecular dynamics study, *Acta Mater.* 77 (2014) 96–110, <https://doi.org/10.1016/j.actamat.2014.04.070>.
- [23] Wei, Dan & Yang, Jie & Dai, Lan-Hong & Wang, Yun-Jiang & Dyre, Jeppe & Douglass, Ian & Harrowell, Peter. (2019). Assessing the utility of structure in amorphous materials. *The Journal of Chemical Physics*. 150. 114502. 10.1063/1.5064531.
- [24] M. Celtek, U. Domekeli, S. Sengul, C. Canan, Effects of Ag or Al addition to CuZr-based metallic alloys on glass formation and structural evolution: A molecular dynamics simulation study, *Intermetallics*, Volume 128, 2021, 107023, <https://doi.org/10.1016/j.intermet.2020.107023>.
- [25] Y.Q. Cheng, E. Ma, H.W. Sheng, Atomic level structure in multicomponent bulk metallic glass, *Phys. Rev. Lett.* 102 (2009) 1–4, <https://doi.org/10.1103/PhysRevLett.102.245501>.
- [26] J. Hwang, Z.H. Melgarejo, Y.E. Kalay, I. Kalay, M.J. Kramer, D.S. Stone, P. M. Voyles, Nanoscale structure and structural relaxation in Zr50Cu45Al5 bulk metallic glass, *Phys. Rev. Lett.* 108 (2012) 195505, <https://doi.org/10.1103/PhysRevLett.108.195505>.
- [27] Kai Liang, Xingguang Zhang, Junwei Qiao, Shaopeng Pan, Shidong Feng, Effects of minor addition of Al and Ag elements on the atomic structure and mechanical property of ZrCu-based metallic glasses, *Journal of Non-Crystalline Solids*, Volume 550, 2020, 120385, <https://doi.org/10.1016/j.jnoncrysol.2020.120385>.
- [28] Deb Nath, S K. (2017). Thermal conductivity and mechanical properties of Zr x Cu 90–x Al 10 under tension using molecular dynamics simulations. *International Journal of Mechanical Sciences*. 144. 10.1016/j.ijmecsci.2017.08.037.